Physics Letters A 375 (2011) 2878–2881

Contents lists available at ScienceDirect

Physics Letters A

www.elsevier.com/locate/pla

Thermoelectric properties of ZnO nanowires: A first principle research

Chaoren Liu *, Jingbo Li

State Key Laboratory for Superlattices and Microstructures, Institute of Semiconductors, Chinese Academy of Sciences, P.O. Box 912, Beijing 100083, China

ARTICLE INFO

Article history:
Received 5 April 2011
Received in revised form 11 June 2011
Accepted 12 June 2011
Available online 14 June 2011
Communicated by R. Wu

Keywords:
Thermoelectric property
ZnO nanowire
First principle calculation
Boltzmann transport equation

ABSTRACT

By means of *ab-initio* electronic structure calculation and one-dimensional Boltzmann transport equation solution, we investigate the size dependent thermoelectric (TE) properties of n-type ZnO nanowires (NWs) and surface passivation effects. As demonstrated by our calculations, largest figure of merit *ZT* achievable in thin NWs is larger than that in wide NWs, whereas being restrained by higher demand of n-type doping. Moreover, bare NWs are superior in TE application comparing with the passivated. To compete with conventional TE materials, lattice thermal conductivity of ZnO NWs should be at least 2 orders of magnitude lower than bulk value.

© 2011 Elsevier B.V. All rights reserved.

1. Introduction

Thermoelectric (TE) materials are regarded as promising candidates in solving energy crisis. However, the complicated interaction between electronic conductivity σ, Seebeck coefficient S and thermal conductivity κ (sum of electron contribution κ_e and lattice contribution κ_l) makes it difficult to enhance the figure of merit $ZT = \sigma S^2 T/(\kappa_e + \kappa_l)$, which has remained around 1.0 for many years. ZT should be increased to no less than 3.0 if we want to put TE materials into application. Lee et al. [1] and Heremans et al. [2] raised ZT by means of distorting density of states (DOS) nearby Fermi level through doping special atoms. Others realized high ZT in complex alloys [3], taking advantage of their low thermal conductivity. Recently, quantum confinement was proposed to be another effective approach [4,5]. On one hand, it is well known that low-dimensional materials have a DOS of sharp shape at band edge [6], which is favorable to high TE efficiency [7]. On the other hand, the large surface to volume ratio in low-dimensional systems intensifies scattering of phonon, decreasing thermal conductivity as a result. It was reported, for example, that the thermal conductivity of silicon NWs was 100 times smaller than bulk value [8,9]. In laboratory, the development of advanced material preparation methods makes it possible to grow NWs with different diameters and surface geometries in different directions, which facilitates the experimental investigation of TE properties in nanomaterials [8,10]. ZnO NWs have received great attention for many years, mostly in their electronic and optical properties [11,12]. To the best of my knowledge, there are no reports related to TE properties in ZnO NWs both experimentally and theoretically.

In this Letter, we utilize a combination of density functional theory (DFT) and Boltzmann transport equation simulation (BTES) to give a description of TE properties in both bare and passivated ZnO NWs, which are [0001] oriented with six $(10\bar{1}0)$ facet surfaces because this is commonest in experiments. Due to the fact that as-prepared ZnO is n-type and p-type doping is difficult in ZnO, we only study the former kind in this Letter. In the first place, we discuss their structural and electronic properties and find that, before passivation, surface Zn atoms relax inward relative to O atoms manifestly, in consequence prolonging NWs in growth direction while, after passivation, the relaxation becomes negligible, which demonstrates our successful dangling bonds saturation. The investigation of TE properties tells that ZT can be tuned up through carrier doping and bare NWs are superior to passivated ones in TE application. Furthermore, ZT can be improved by decreasing NWs dimension, along with an increasing requirement of free electron doping.

2. Calculation method

Two bare NWs, with hexagonal cross sections and different diameters (3.69 Å and 9.78 Å), are constructed from LDA relaxed wurtzite bulk ZnO ($a = 3.24$ Å, $c = 5.23$ Å, $u = 0.387$) and labeled as B1 and B2. Then we saturate the dangling bonds on B1 and B2 with pseudo-hydrogen atoms, which have equal amount of nucleus and electron charge, and label the counterparts as P1 and P2 respectively. Each dangling bond on surface Zn atoms is terminated with one H1.5 atom, whose charge amount is $1.5e$ ($e = 1.6 \times 10^{-19}$ C), while each dangling bond on surface O atoms

---

* Corresponding author. Tel.: +86 0 15811043227; fax: +86 10 82305056.
E-mail addresses: supermanliu5@semi.ac.cn (C. Liu), jbli@semi.ac.cn (J. Li).

0375-9601/$ – see front matter © 2011 Elsevier B.V. All rights reserved.
doi:10.1016/j.physleta.2011.06.024

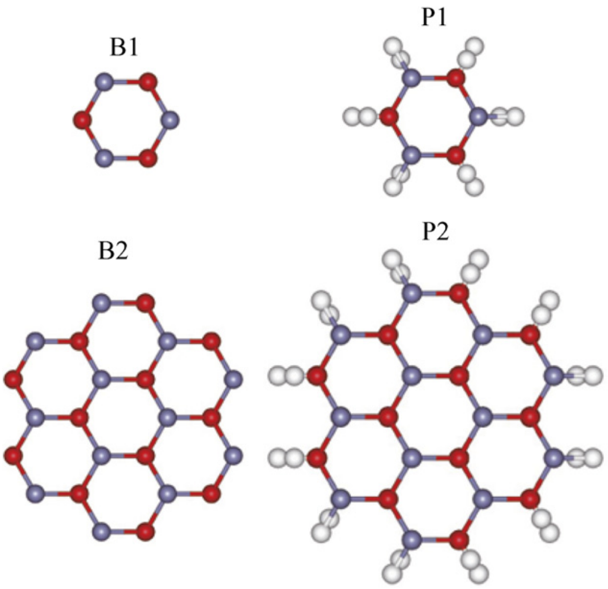

Fig. 1. (Color online.) Views of as-constructed B1, B2, P1 and P2 in [0001] direction. Zn, O and pseudo-hydrogen atoms are represented as blue, red and gray balls.

with one H0.5, whose charge amount is 0.5*e*. The bond lengths of Zn–H1.5 and O–H0.5 are assumed to be the same as in ZnH_2 and H_2O. We put the views of all NWs in Fig. 1 in [0001] direction. The initial structures are then relaxed with quasi-Newton algorithm until Hellmann–Feynman force acting on each atom is smaller than 0.01 eV/Å. We allow the lattice constant *c* to change freely since we find that ZnO [0001] NWs tend to stretch after relaxation. The periodic boundary condition is applied and NWs are separated by 10 Å vacuum layers, which proves sufficient to eliminate the interaction between different images. The atomistic relaxation and electronic structure calculation are performed with density functional theory (DFT) as implemented in VASP code [13]. Local density approximation (LDA) is utilized to treat exchange-correlation energy. Frozen-core projected augmented wave methods [14] is utilized to describe the ion–electron interactions. Zn3*d* electrons are explicitly treated as valence electrons. Monkhorst–Pack special *k*-point grid $(1 \times 1 \times 8)$ is used to integrate in Brillouin zone.

The electronic conductivity σ, Seebeck coefficient *S* and electronic thermal conductivity κ_e are obtained by means of processing electronic structures with the solution of one-dimensional Boltzmann transport equation in constant relaxation time approximation [7]:

$$\sigma = e^2 \int_{-\infty}^{+\infty} d\varepsilon \left(-\frac{\partial f_0}{\partial \varepsilon}\right) \sum(\varepsilon), \tag{1}$$

$$T\sigma S = e \int_{-\infty}^{+\infty} d\varepsilon \left(-\frac{\partial f_0}{\partial \varepsilon}\right) \sum(\varepsilon)(\varepsilon - \mu), \tag{2}$$

$$T\kappa_0 = \int_{-\infty}^{+\infty} d\varepsilon \left(-\frac{\partial f_0}{\partial \varepsilon}\right) \sum(\varepsilon)(\varepsilon - \mu)^2, \tag{3}$$

$$\sum(\varepsilon) = \sum_{\vec{k}} \nu_x(\vec{k})^2 \tau(\vec{k}) \delta\big(\varepsilon - \varepsilon(\vec{k})\big), \tag{4}$$

$$\kappa_e = \kappa_0 - T\sigma S^2, \tag{5}$$

where *e* is charge of electron; μ is chemical potential; *T* is absolute temperature; f_0 is Fermi distribution function; $\nu_x(\vec{k}) = (1/\hbar)(\partial E(\vec{k})/\partial k_x)$; τ is relaxation time. τ varies with different electronic structures, carrier concentrations, temperatures and so on, which makes it too complex to be obtained precisely. For lack of experimental dependence of electronic mobility on carrier concentration in ZnO NWs, we obtain the relaxation time in NWs by fitting the calculated electronic mobility in bulk ZnO to experimental values [15]. This approximation has been testified reasonable by Shi et al. [16] and Vo et al. [17] if we just care about the qualitative tendency rather than the accuracy of results.

Table 1
LDA bandgap and effective mass ([0001] direction) of B1, B2, P1 and P2.

	B1	B2	P1	P2	Bulk
E_g (eV)	1.99	1.47	4.05	2.16	0.79
m^* (m_e)	0.350	0.295	0.855	0.395	0.181[a]

[a] See Ref. [20].

3. Structural and electronic properties

We start by investigating the structural properties of bare and passivated ZnO NWs. Since the relaxation of NWs with different diameters follows similar trend, we take B2 and P2 as the example. Surface Zn atoms move inward relative to outmost O atoms, resulting in a distorted hexagonal cross section with three sides short (4.65 Å) and three sides long (5.93 Å). To release stress, NWs stretch in growth direction, with lattice constant *c* of B2, for example, increasing from bulk value 5.23 Å to 5.41 Å. The angle of surface O–Zn–O, in view of [0001] direction, increases to 140° from 120° while that of Zn–O–Zn decreases to 114°. A similar result has been reported by Xiang et al. [18] and Xu et al. [19]. After pseudo-hydrogen passivation, we find that the relaxation of surface atoms becomes unnoticeable, which demonstrates our success of surface state elimination. The bond length of Zn–H1.5 and O–H0.5 are relaxed to 1.64 Å and 1.05 Å, close to the values in ZnH_2 (1.62 Å) and H_2O (0.94 Å).

All ZnO NWs studied in this Letter prove to be semiconducting with direct bandgap at Γ point, which are shown in Table 1. We can see that bandgap increases when NW diameter decreases and all of them are larger than the bulk value. Passivation process enlarges the bandgap further. To understand these phenomena, we analyze the composition of bands and draw the charge density of valence band maximum (VBM) and conduction band minimum (CBM) in Fig. 2. VBM of bare NWs are contributed by Zn3*d* and O2*p* orbits, however of surface atoms, which indicates surface states, while CBM mainly consist of Zn4*s* orbits from inside atoms, which indicates bulk states. All of these are verified further in Fig. 2 (b1) and (c1). As indicated by Xiang [18], the O2*p*-like surface state in B2 is only 80 meV above the VBM of bulk ZnO. In this case, when diminishing the diameter of bare NWs, quantum confinement effect will uplift CBM significantly because bulk state delocalizes greatly in radial direction. However, surface state responses to dimension constraint inertly due to its localized attribute. Hence the delocalized property of CBM as well as the low position of surface state result in a sensitive size-dependent bandgap of bare NW and a sharp increase of bandgap from bulk to NWs. In P1 and P2, Zn3*d* and O2*p* orbits in core part are the main component of VBM while CBM is primarily contributed by Zn4*s* and O3*s* orbits of inside atoms. From Fig. 2 (b2) and (c2), it is shown that the charge of both VBM and CBM locates mainly in inner part, which demonstrates their bulk state attributes. That is to say dangling bonds termination with pseudo-hydrogen successfully eliminates the surface states nearby VBM, meanwhile enlarging bandgap. Moreover, it is easy to notice that difference between the bandgap of B2 and B1 is 0.52 eV but the value for P2 and P1 is as large as 1.89 eV, which could be understood as follows. CBM might become more delocalized in radial direction after surface passiva-

Download English Version:

https://daneshyari.com/en/article/1867170

Download Persian Version:

https://daneshyari.com/article/1867170

Daneshyari.com